

# FORMATION OF DWARF SPHEROIDAL GALAXIES VIA MERGERS OF DISKY DWARFS

STELIOS KAZANTZIDIS<sup>1</sup>, EWA L. ŁOKAS<sup>2</sup>, LUCIO MAYER<sup>3</sup>, ALEXANDER KNEBE<sup>4</sup>, AND JAROSŁAW KLIMENTOWSKI<sup>2</sup>

*Accepted by ApJL on September 7, 2011*

## ABSTRACT

We perform collisionless  $N$ -body simulations to investigate whether binary mergers between rotationally-supported dwarfs can lead to the formation of dwarf spheroidal galaxies (dSphs). Our simulation campaign is based on a hybrid approach combining cosmological simulations and controlled numerical experiments. We select merger events from a Constrained Local Universe (CLUES) simulation of the Local Group (LG) and record the properties of the interacting dwarf-sized halos. This information is subsequently used to seed controlled experiments of binary encounters between dwarf galaxies consisting of exponential stellar disks embedded in cosmologically-motivated dark matter halos. These simulations are designed to reproduce eight cosmological merger events, with initial masses of the interacting systems in the range  $\sim (5 - 60) \times 10^7 M_\odot$ , occurring quite early in the history of the LG, more than 10 Gyr ago. We compute the properties of the merger remnants as a distant observer would and demonstrate that at least three of the simulated encounters produce systems with kinematic and structural properties akin to those of the classic dSphs in the LG. Tracing the history of the remnants in the cosmological simulation to  $z = 0$ , we find that two dSph-like objects remain isolated at distances  $\gtrsim 800$  kpc from either the Milky Way or M31. These systems constitute plausible counterparts of the remote dSphs Cetus and Tucana which reside in the LG outskirts, far from the tidal influence of the primary galaxies. We conclude that merging of rotationally-supported dwarfs represents a viable mechanism for the formation of dSphs in the LG and similar environments.

*Subject headings:* galaxies: dwarf – galaxies: Local Group – galaxies: fundamental parameters – galaxies: kinematics and dynamics – methods: numerical

## 1. INTRODUCTION

The origin of dwarf spheroidal galaxies (dSphs) in the Local Group (LG) is a long-standing subject of debate. These intriguing systems are the faintest galaxies known (e.g., Mateo 1998) and they are believed to be highly dark matter (DM) dominated (e.g., Mateo 1998; Łokas 2009; Walker et al. 2009). Moreover, dSphs are gas poor or completely devoid of gas (e.g., Greulich & Putman 2009) and they are characterized by pressure-supported, spheroidal stellar components (e.g., Mateo 1998) and a wide diversity of star formation histories (e.g., Grebel 2000). While our understanding of dSphs has grown impressively in the past decade, a definitive model for their formation still remains elusive.

One class of models attempts to explain the origin of dSphs via various environmental mechanisms, including tidal and ram pressure stripping (e.g., Einasto et al. 1974; Faber & Lin 1983; Mayer et al. 2001; Kravtsov et al. 2004; Mayer et al. 2006, 2007; Klimentowski et al. 2009; Kazantzidis et al. 2011) and resonant stripping (D’Onghia et al. 2009). In this context, the tidal stirring model (Mayer et al. 2001) posits the formation of dSphs via the tidal interactions between rotationally-supported dwarfs and Milky Way (MW)-

sized host galaxies. While this model naturally explains the tendency of dSphs to be concentrated near the dominant spirals, it is challenged by the presence of the isolated dSphs Cetus and Tucana in the LG outskirts. Such examples illustrate the need for complementary models concerning the origin of dSphs.

In the current galaxy formation paradigm (e.g., White & Rees 1978), the quiescent cooling of gas within a virialized DM halo results in the formation of a rotationally-supported disk of stars. Thus, any scenario for dSph formation must incorporate physical processes for transforming initially rotationally-supported stellar systems to ones dominated by random motions. Interactions and mergers between galaxies may constitute such a mechanism. Indeed, on larger scales, the tidal heating and violent relaxation associated with mergers of massive, disk galaxies effectively destroy the stellar disks creating a kinematically hot, pressure-supported spheroid that resembles an elliptical galaxy (e.g., Barnes 1992). It has also been demonstrated that encounters between dwarf halos can lead to their very strong evolution (e.g., Knebe et al. 2006; Klimentowski et al. 2010). Klimentowski et al. (2010) reported in their constrained DM cosmological simulation of the LG that a few percent of all surviving subhalos had undergone a substantial encounter with another dwarf halo in the past. Most of these events occurred early in the LG history and before the dwarf halos were accreted and became satellites of either the MW or M31. Therefore, although the great majority of LG dwarf galaxies should not have participated in mergers with other dwarfs in the past, at least some of them may have experienced such interactions.

Motivated by these findings, we selected eight merger

<sup>1</sup> Center for Cosmology and Astro-Particle Physics; and Department of Physics; and Department of Astronomy, The Ohio State University, Columbus, OH 43210, USA; stelios@mps.ohio-state.edu

<sup>2</sup> Nicolaus Copernicus Astronomical Center, 00-716 Warsaw, Poland

<sup>3</sup> Institute for Theoretical Physics, University of Zürich, CH-8057 Zürich, Switzerland

<sup>4</sup> Grupo de Astrofísica, Departamento de Física Teórica, Módulo C-8, Universidad Autónoma de Madrid, Cantoblanco E-28049, Spain

events from the same LG simulation and re-simulated them at higher resolution, embedding stellar disks inside the dwarf DM halos. Our goal is to determine whether mergers of initially rotationally-supported dwarfs can produce systems with kinematic and structural properties akin to those of the classic LG dSphs.

## 2. METHODS

The basis for our experiments is a constrained DM cosmological simulation of the Local Universe which reproduces the main LG properties at  $z = 0$ . This simulation (see Klimentowski et al. 2010) is part of the CLUES project<sup>5</sup> (Gottlöber et al. 2010). We identify dwarf-sized halos participating in mergers and record their properties by utilizing the halo catalogues of the cosmological simulation that were generated with the AMIGA halo finder (AHF) (Knollmann & Knebe 2009).

In practice, it is not feasible to simulate all possible encounters identified in the halo catalogues at sufficient numerical resolution. For our purposes, it would be sufficient to show that even a single *representative* merger between dwarf galaxies can lead to the formation of a dSph. To this end, we selected eight *binary* interactions, which we denote M1-M8, for subsequent re-simulation. These encounters corresponded to mass ratios of the interacting systems ranging approximately from 1:1 to 1:4. While these merger events were not chosen in any special way, they were associated with a significant mass transfer between the systems ( $\gtrsim 80\%$ ) indicating the occurrence of an actual merger, as opposed to a weak encounter or a fly-by.

Table 1 contains the properties of the two interacting systems in each case. Column 2 lists the redshifts at which the mergers were identified in the cosmological simulation. All recorded encounters took place at very early cosmic times ( $z \gtrsim 2.5$ ), in accordance with the expectation for the epoch of rapid growth of low-mass halos (e.g., Wechsler et al. 2002). We note that these mergers occurred before the dwarf halos have been accreted onto more massive structures. Indeed, subsequent to accretion, the merging probability of halos diminishes due to the large host velocity dispersion (e.g., De Lucia et al. 2004).

Columns 3-6 list the halo virial parameters ( $M_{\text{vir}}$ ,  $R_{\text{vir}}$ ,  $V_{\text{vir}}$ ) and concentrations  $c \equiv R_{\text{vir}}/r_s$  (where  $r_s$  denotes the “scale radius” where the product  $\rho(r)r^2$  reaches its maximum value). Columns 7-10 list the dimensionless spin parameters  $\lambda$  (e.g., Peebles 1969) and the direction of the angular momentum vector of the dwarf halos normalized to unity.

We constructed numerical realizations of dwarfs using the method described in Kazantzidis et al. (2005). The models consisted of exponential stellar disks embedded in cosmologically-motivated Navarro et al. (1996) DM halos whose properties match those of the cosmological halos in Table 1. We parametrized the mass of the stellar disk as a fraction,  $f_d$ , of the halo  $M_{\text{vir}}$  and the disk thickness as  $z_d/R_d$  ( $z_d$  and  $R_d$  denote the disk vertical scale height and radial scale length, respectively). For simplicity, we fix the values of  $z_d/R_d$  and  $f_d$  in all models. In our modeling,  $R_d$  is determined by  $M_{\text{vir}}$ ,  $\lambda$ ,  $c$ , and  $f_d$  via the semi-analytic model of Mo et al. (1998) for the for-

mation of disks<sup>6</sup>. The resulting  $R_d$  are listed in column 11 of Table 1.

We take the expectation that dwarf galaxies should be born as thick, puffy systems (e.g., Kaufmann et al. 2007) into account by conservatively adopting  $z_d/R_d = 0.2$ . Moreover, we choose  $f_d = 0.005$ . Such small value is consistent with that inferred for some of the faintest LG dwarf irregular galaxies (dIrrs) such as Leo A (Brown et al. 2007) and SagDIG (Young & Lo 1997). Assuming an isothermal DM halo, the velocity dispersions of these systems ( $\sigma \sim 10 \text{ km s}^{-1}$ ) correspond to  $V_{\text{vir}} \sim 14 \text{ km s}^{-1}$ , comparable to those of our halos. Tiny stellar components are expected in such low-mass systems because both gas accretion/retention and star formation would be strongly suppressed by re-ionization and supernovae driven outflows (e.g., Mayer 2010). Oh et al. (2011) computed  $f_d$  for a fairly large sample of dwarfs in the THINGS survey, obtaining values  $\sim 0.01$ , albeit for galaxies that would have been less affected by the aforementioned effects having rotational velocities that are a factor of 2 – 3 larger than those considered here.

We rotated each dwarf model so that the direction of the angular momentum vector of its DM halo was identical to that of the corresponding cosmological halo. In our modeling, the angular momentum of the disk is aligned with that of the host DM halo. This results in relative orientations of the disk angular momenta that span a wide range ( $\sim 10^\circ - 120^\circ$ ). Lastly, we realized the merger simulations using the initial positions and velocities of the corresponding cosmological halos with respect to their center of mass (Table 2).

All merger simulations were performed with the  $N$ -body code PKDGRAV (Stadel 2001). Each  $N$ -body dwarf model contained  $N_h = 3 \times 10^5$  DM particles and  $N_d = 5 \times 10^4$  disk particles. The gravitational softening was set to  $\epsilon_h = 30 \text{ pc}$  and  $\epsilon_d = 15 \text{ pc}$ , respectively. Force resolution was adequate to resolve all scales of interest.

## 3. RESULTS

All merger products were allowed to reach equilibrium before any analysis was performed. We first determined the principal axes of the stellar components using the moments of the inertia tensor. Subsequently, we produced 2D maps of the stellar surface distribution and kinematics along the three principal axes and “observed” the merger remnants as a distant observer would.

Given that observed dSphs are supported by random motions (e.g., Mateo 1998), only remnants satisfying  $V_{\text{rot}}/\sigma_* \lesssim 1$  (where  $V_{\text{rot}}$  and  $\sigma_*$  denote the stellar rotational velocity and the one-dimensional, central velocity dispersion, respectively) may be regarded as dSphs. Using the kinematic maps of the stellar mean radial velocity and velocity dispersion, we computed  $V_{\text{rot}}/\sigma_*$  for all remnants. For each line-of-sight, the value of  $V_{\text{rot}}$  corresponded to the maximum velocity found anywhere on the map. For the velocity dispersion  $\sigma_*$  we adopted the central value.

<sup>6</sup> We note that the Mo et al. (1998) formalism may be inappropriate for dwarf galaxies at high-redshift. However, given the lack of knowledge for the structure of dwarf galaxies at early cosmic times, utilizing the Mo et al. (1998) model constitutes a reasonable alternative to assigning arbitrary values to the disk scale lengths of our dwarfs.

<sup>5</sup> <http://www.clues-project.org>

TABLE 1  
INITIAL PROPERTIES OF MERGING DWARFS

Merger (1)	$z$ (2)	$M_{\text{vir}}$ ( $10^7 M_{\odot}$ ) (3)	$R_{\text{vir}}$ (kpc) (4)	$V_{\text{vir}}$ (km/s) (5)	$c$ (6)	$\lambda$ (7)	$L_x$ (8)	$L_y$ (9)	$L_z$ (10)	$R_d$ (pc) (11)
M1	3.02	6.51	3.15	9.43	4.48	0.046	-0.34	0.73	-0.59	119
		5.99	3.03	9.22	3.08	0.032	-0.21	-0.22	-0.95	97
M2	3.82	7.31	2.69	10.82	4.11	0.039	-0.18	-0.41	-0.89	92
		7.17	2.67	10.75	1.92	0.033	-0.70	0.68	0.21	103
M3	6.67	5.78	1.56	12.61	1.97	0.054	-0.05	-0.86	-0.50	90
		7.34	1.69	13.66	1.46	0.047	-0.11	-0.76	-0.64	94
M4	3.15	58.37	6.24	20.05	1.34	0.032	0.74	0.64	-0.20	257
		19.95	4.36	14.03	1.13	0.067	0.25	0.91	-0.32	340
M5	3.82	14.76	3.41	13.65	2.92	0.034	-0.68	0.13	-0.72	117
		8.21	2.79	11.26	2.61	0.065	-0.37	0.81	0.47	171
M6	3.82	24.96	4.04	16.30	1.67	0.051	0.80	0.21	0.56	231
		22.38	3.89	15.72	4.10	0.032	-0.48	0.88	0.02	112
M7	2.57	5.15	3.00	8.59	3.09	0.045	-0.54	-0.79	-0.31	128
		21.06	5.16	13.25	2.30	0.077	0.97	0.03	-0.16	378
M8	3.02	41.84	5.77	17.65	6.25	0.026	0.75	-0.62	-0.27	116
		34.18	5.39	16.52	5.88	0.031	0.99	-0.07	0.09	130

TABLE 2  
INITIAL POSITIONS AND VELOCITIES OF MERGING DWARFS

Merger	$x$ (kpc)	$y$ (kpc)	$z$ (kpc)	$V_x$ (km/s)	$V_y$ (km/s)	$V_z$ (km/s)
M1	-16.69	-17.68	-4.84	4.84	1.99	0.70
	18.15	19.22	5.26	-5.26	-2.16	-0.76
M2	-6.67	0.29	-3.13	5.52	2.36	1.73
	6.78	-0.30	3.19	-5.63	-2.40	-1.76
M3	4.78	-0.04	-0.23	-0.64	-4.18	1.85
	-3.76	0.03	0.18	0.50	3.29	-1.46
M4	-1.96	-3.30	0.54	-3.04	0.19	0.68
	5.74	9.65	-1.58	8.89	-0.56	-2.00
M5	-0.02	2.06	0.18	-1.10	-6.38	1.74
	0.04	-3.70	-0.32	1.97	11.47	-3.13
M6	4.58	6.34	3.75	-3.33	1.99	-3.61
	-5.11	-7.07	-4.18	3.71	-2.21	4.02
M7	1.49	2.23	6.13	-0.54	-20.50	-5.27
	-0.36	-0.57	-1.50	0.13	5.01	1.29
M8	-7.76	-3.02	-5.87	4.54	-6.91	-1.21
	9.50	3.70	7.18	-5.56	8.46	1.48

Most classic dSphs have projected ellipticities,  $\epsilon \equiv 1 - b/a$  (where  $b$  and  $a$  denote the projected minor and major axis of the stellar distribution, respectively) in the range

$0.1 \lesssim \epsilon \lesssim 0.5$  (e.g., Mateo 1998; McGaugh & Wolf 2010). Therefore, we classify as dSphs only those remnants that satisfy  $\epsilon \lesssim 0.5$ . For each line-of-sight, we measured  $\epsilon$  at a distance of  $2r_{1/2}$ , where  $r_{1/2}$  is the half-light radius. Such distances are consistent with those adopted in observational studies (e.g., McConnachie & Irwin 2006).  $r_{1/2}$  were determined by calculating the radius containing half the total number of stars in the surface density distribution of each remnant. The range of  $r_{1/2}$  in Table 3 corresponds to the minimum and maximum values determined for the lines of sight along the three principal axes and reflects the fact that the remnants are not spherical. Figure 1 shows the surface density maps of all eight merger remnants.

Columns 3-5 of Table 3 list the range of values of  $V_{\text{rot}}/\sigma_*$  and  $\epsilon$  for each remnant together with the outcome of the classification scheme based on the two criteria above. Any random line-of-sight would correspond to values of  $V_{\text{rot}}/\sigma_*$  and  $\epsilon$  within the ranges quoted in Table 3.

Out of eight initial merger remnants, three (M3, M6, and M8) would be classified as bona fide dSphs. If we slightly relax the shape criterion above by considering the most elongated classic dSph Ursa Minor with  $\epsilon \approx 0.6$  (Mateo 1998), then seven of our remnants would qualify as dSphs (we indicate this by using the notation "dSph?" in column 5 of Table 3 to characterize remnants M1, M2, M5, and M7). As in mergers between massive disk galaxies (e.g., Cox et al. 2006), the values of  $V_{\text{rot}}/\sigma_*$  are affected by both the mass ratios of the merging systems and the degree of initial alignment of the disks' angular momenta. Indeed, despite the near alignment of the disk spins in M8, a dSph does form. This is because the disks

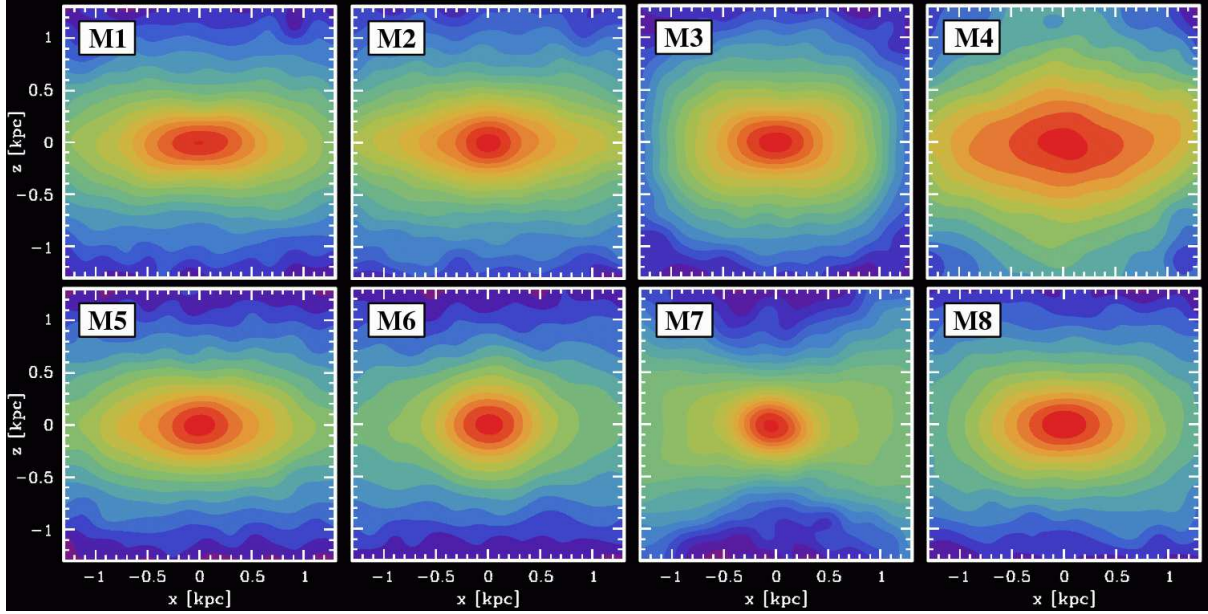


FIG. 1.— Surface number density distribution of stars in the merger remnants. Results are presented for the most non-spherical views along the intermediate axis of the stellar distribution,  $y$  (where  $x$  and  $z$  denote the major and minor axes, respectively). The stars were binned into  $0.2 \text{ kpc} \times 0.2 \text{ kpc}$  fields perpendicular to the line-of-sight. The contours correspond to the number of stars  $N$  within such a bin and are equally spaced by 0.2 in  $\log N$ . The innermost contours are in the range  $\log N = 3.2 - 4.2$  depending on the remnant.

TABLE 3  
PROPERTIES OF MERGER REMNANTS

Merger (1)	$r_{1/2}$ (kpc) (2)	$V_{\text{rot}}/\sigma_*$ (3)	$\epsilon \equiv 1 - b/a$ (4)	Classification (5)	$M_V$ (mag) (6)	$\mu_V$ (mag arcsec $^{-2}$ ) (7)	Color in Figure 2 (8)
M1	0.22-0.40	0.10-0.20	0.11-0.63	dSph?	-(8.3-9.2)	25.1-27.1	green
M2	0.22-0.38	0.09-0.69	0.04-0.59	dSph?	-(8.5-9.4)	24.9-26.6	red
M3	0.24-0.32	0.12-0.70	0.14-0.45	dSph	-(8.4-9.3)	25.0-26.7	blue
M4	1.24-1.50	0.19-1.88	0.12-0.50	non-dSph	-(10.3-11.2)	26.4-27.6	black
M5	0.30-0.52	0.20-0.60	0.03-0.59	dSph?	-(9.0-9.9)	25.1-26.8	orange
M6	0.42-0.60	0.22-0.75	0.06-0.50	dSph	-(9.7-10.7)	24.7-26.1	magenta
M7	0.28-0.38	0.33-0.92	0.08-0.54	dSph?	-(9.1-10.0)	24.4-25.9	cyan
M8	0.29-0.41	0.09-0.50	0.07-0.47	dSph	-(10.3-11.2)	23.7-25.3	brown

are effectively destroyed in this nearly equal-mass encounter. On the other hand, mergers M4 and M7 which correspond to the smallest mass ratios produce remnants that exhibit the highest values of  $V_{\text{rot}}/\sigma_*$ . In these cases, the remnants maintain part of the original rotation of the more massive disks which were not completely destroyed by the encounters. Moreover, although M7 corresponds to a smaller mass ratio compared to M4, its remnant exhibits a lower value of  $V_{\text{rot}}/\sigma_*$  and is classified as a dSph. This is because the intrinsic spins of the disks in this case are oriented almost in the opposite direction, whereas the disk spins are nearly aligned in M4.

Columns 6 and 7 of Table 3 list the absolute magnitude in the V-band,  $M_V$ , and the central surface brightness,  $\mu_V$ . For simplicity, the magnitudes were determined by assuming that our imaginary observer will be able to detect all stars. The total stellar masses were translated into luminosities assuming a stellar mass-to-light ratio of  $M_*/L_V = (2.5 \pm 1)M_\odot/L_\odot$ . The mean value is

the *present-time* prediction for a single, low-metallicity stellar population in the standard model described by Bruzual & Charlot (2003). The lower limit roughly corresponds to the mean  $M_*/L_V$  for pressure-supported LG dwarfs estimated from resolved stellar population studies (e.g., Mateo 1998). The  $1M_\odot/L_\odot$  variation addresses some of the uncertainty regarding our assumptions for the mean  $M_*/L_V$  above and the lack of relevant physical processes in the simulations (e.g., star formation) and illustrates how the predicted magnitudes may vary due to unknown  $M_*/L_V$ .

Lastly,  $\mu_V$  were computed by considering stars within  $0.2 r_{1/2}$  from the center of each remnant. Such distances roughly correspond to the innermost data points of surface brightness distributions of observed dwarfs (e.g., McConnachie & Irwin 2006). The ranges of  $\mu_V$  in column 7 of Table 3 include both the variation of  $r_{1/2}$  and the uncertainty in  $M_*/L_V$ .

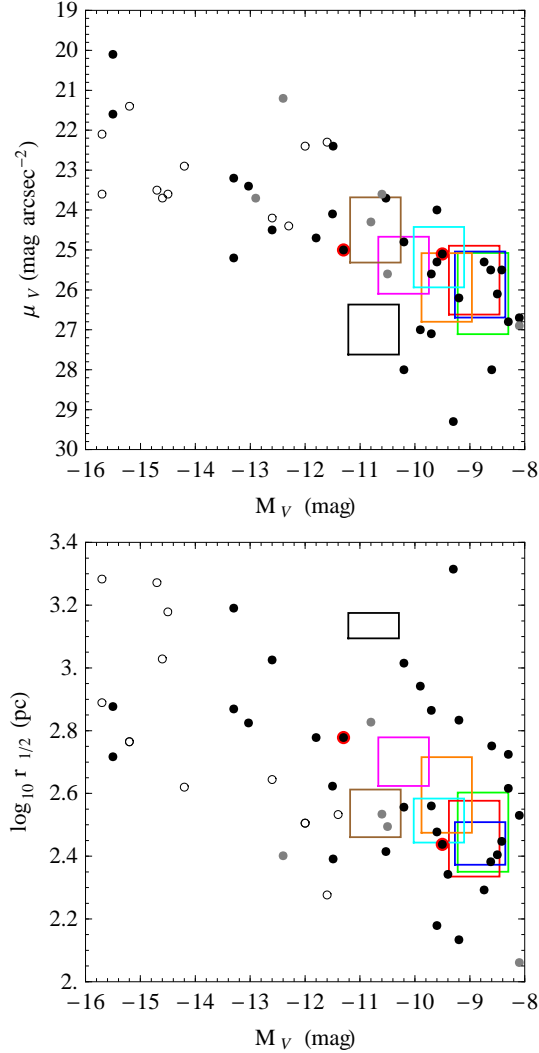


FIG. 2.— Absolute magnitude,  $M_V$ , versus central surface brightness,  $\mu_V$  (upper panel) and  $M_V$  versus projected half-light radius,  $r_{1/2}$  (bottom panel) for dwarf galaxies. The merger remnants correspond to color rectangles whose sizes indicate the ranges of values in Table 3. Symbols show results for observed LG dwarfs: open symbols correspond to dIrrs, filled black symbols show results for both dSph and dwarf spheroidal/dwarf elliptical (dSph/dE) systems, and filled gray symbols correspond to “transition-type” (dIrr/dSph) dwarfs. Isolated dSphs Cetus and Tucana are additionally marked with red circles. All data for observed dwarfs are taken from Table 2 of Lokas et al. (2011). The remnants that would be classified as dSphs and the LG classic dSphs occupy essentially the same regions on both planes.

#### 4. DISCUSSION

Galaxies can be characterized by correlations between their fundamental parameters. This also applies to LG dwarf galaxies which occupy characteristic regions in the  $M_V - \mu_V$  and  $M_V - r_{1/2}$  planes (e.g., Tolstoy et al. 2009). Figure 2 illustrates how our merger remnants (colored rectangles) compare with the population of LG dwarf galaxies (symbols) in these two planes. Except M4 which is not classified as a dSph, our merger products and the LG classic dSphs (filled black symbols) occupy essentially the same regions on the  $M_V - \mu_V$  and  $M_V - r_{1/2}$  planes. This further suggests that merging between rotationally-

supported dwarfs constitutes a viable mechanism for the formation of dSphs.

Using the subhalo catalogues we have traced the history of the merger remnants in the cosmological simulation to  $z = 0$ . From the seven systems that could be classified as dSphs, four (M2, M3, M6, and M7) survived as individual entities to the present-time. Two of the remaining merger products (M1 and M8) were accreted by a factor of  $\sim 100$  more massive halos, while M5 participated in a 1:5 interaction with a more massive object. Interestingly, all four merger remnants that have survived as individual entities to  $z = 0$  appear to be remote, located in the periphery of the simulated LG at distances  $\gtrsim 800$  kpc from either the MW or M31. These systems constitute plausible counterparts of the oddly isolated dSphs Cetus and Tucana which reside in the LG outskirts, the former at a distance of  $\sim 800$  kpc from the MW (e.g., McConnachie et al. 2005) while the latter at  $\sim 1300$  kpc from M31 (e.g., Saviane et al. 1996). The observational parameters of Tucana ( $M_V = -9.5$  mag,  $r_{1/2} = 274$  pc,  $\mu_V = 25.1$  mag arcsec $^{-2}$ ,  $V_{\text{rot}}/\sigma_* \sim 1$ , and  $\epsilon = 0.48$ ; Table 2 of Lokas et al. 2011) are in reasonable agreement with those of dSphs M3 and M8 in Table 3<sup>7</sup>. On the other hand, the Cetus dwarf ( $M_V = -11.3$  mag,  $r_{1/2} = 600$  pc,  $\mu_V = 25.0$  mag arcsec $^{-2}$ ,  $V_{\text{rot}}/\sigma_* = 0.45$ , and  $\epsilon = 0.33$ ; Table 2 of Lokas et al. 2011) is brighter and more extended and therefore more akin to our dSph M6. Overall, the agreement is particularly noteworthy because our simulation program did not aim to reproduce the properties of these objects.

The evolutionary scenario proposed here may also be relevant for the relatively isolated transitional (dIrr/dSph) dwarfs Phoenix, LGS3, and Pegasus (Mateo 1998) that usually differ from dSphs only in the presence of small amounts of gas, and even for the remote peculiar dwarf galaxy VV124 (Kopylov et al. 2008).

Alternative models exist for explaining the puzzling presence of Tucana and Cetus in the outskirts of the LG. For example, as a result of three-body interactions, satellites can acquire extremely energetic orbits with apocenters beyond the  $R_{\text{vir}}$  of the primary and be ejected to large distances (Sales et al. 2007; Ludlow et al. 2009). In this model, ejected subhalos are typically the least massive members of a group of satellites that is tidally disrupted by the host. Tidal interactions with the more massive companions within the groups may already transform the eventually ejected dwarfs into dSphs, via either tidal stirring, perhaps enhanced by resonances (D’Onghia et al. 2009), or mergers. Ongoing investigations of the stellar components of Tucana and Cetus (e.g., Bernard et al. 2009; Monelli et al. 2010a), including their star formation histories (e.g., Monelli et al. 2010b), may soon provide constraints on the various competing models for their origin.

Lastly, our simulations neglect gas dissipation and star formation. Dwarf galaxies are known to be gas rich at least at low redshift (e.g., Geha et al. 2006). Although such dissipative processes should be important in encounters of massive galaxies with cold gas disks (e.g., Kazantzidis et al. 2005), they should have a

<sup>7</sup> Due to the very large distances involved the detection of rotation at such high levels for Tucana should be regarded as tentative and needs to be confirmed by future observations.

rather marginal effect in our case. Indeed, the dwarf halos considered here (Table 1) have both low  $V_{\text{vir}} < 20 \text{ km s}^{-1}$  and concentrations ( $1 \lesssim c \lesssim 6.5$ ), implying maximum circular velocities  $V_{\text{max}}$  only slightly above  $V_{\text{vir}}$ . Kaufmann et al. (2007) have shown that halos with  $V_{\text{max}} < 35 \text{ km s}^{-1}$  would not host thin gaseous disks but rather spheroidal gas distributions.

Furthermore, neglecting self-shielding, Mayer et al. (2006) have shown that the gas in dwarf halos would still be heated to  $T > 10^4 \text{ K}$  by the cosmic ionizing background at  $z > 2$ , when all of our mergers occur. Given that  $V_{\text{vir}} \sim 20 \text{ km s}^{-1}$  corresponds to  $T_{\text{vir}} \sim 10^4 \text{ K}$ , the gas distribution would form an extended pressure-supported envelope. Depending on halo mass, this envelope would be barely confined by the halo potential, or even be completely evaporated from the halo (Barkana & Loeb 1999). Regardless, the gas component would not remain confined into the central disk, except perhaps near the very center where self-shielding might be sufficient to preserve a tiny fraction of cold dense gas (Susa & Umemura 2004). Therefore, either the mergers would occur essentially in a dissipationless regime, as we have assumed here, or they would contain a tenuous hot atmosphere which could be shock heated further as a result of the merger (e.g., Kazantzidis et al. 2005) and become unbound thereafter in the absence of efficient cooling. In either case, no gas inflows and no appreciable triggered star formation would occur, contrary

to what happens in mergers of massive galaxies (e.g., Barnes & Hernquist 1996). In summary, the effects of gas and star formation on the structure of the merger remnants are expected to be weak. Therefore, although they will have to be confirmed with hydrodynamical simulations, the qualitative arguments outlined above suggest that our collisionless experiments have likely captured the essence of the morphological evolution in mergers of disk dwarf galaxies.

The authors would like to thank the referee, Matteo Monelli, for constructive comments on the manuscript and the CLUES members S. Gottlöber, Y. Hoffman, and G. Yepes for providing the LG simulation. We also acknowledge stimulating discussions with Jürg Diemand, Alan McConnachie, Chris Orban, and David Weinberg. S.K. is supported by the Center for Cosmology and Astro-Particle Physics at The Ohio State University. This research was partially supported by the Polish National Science Centre under grant N N203 580940. A.K. is supported by the Ministerio de Ciencia e Innovación (MICINN) in Spain through the Ramon y Cajal program and further acknowledges support from grants AYA 2009-13875-C03-02, AYA2009-12792-C03-03, and CAM S2009/ESP-1496. This research was also supported by the Ohio Supercomputer Center (<http://www.osc.edu>).

## REFERENCES

- Barkana, R. & Loeb, A. 1999, *ApJ*, 523, 54  
 Barnes, J. E. 1992, *ApJ*, 393, 484  
 Barnes, J. E. & Hernquist, L. 1996, *ApJ*, 471, 115  
 Bernard, E. J. et al. 2009, *ApJ*, 699, 1742  
 Brown, W. R., Geller, M. J., Kenyon, S. J., & Kurtz, M. J. 2007, *ApJ*, 666, 231  
 Bruzual, G. & Charlot, S. 2003, *MNRAS*, 344, 1000  
 Cox, T. J., Dutta, S. N., Di Matteo, T., Hernquist, L., Hopkins, P. F., Robertson, B., & Springel, V. 2006, *ApJ*, 650, 791  
 De Lucia, G., Kauffmann, G., Springel, V., White, S. D. M., Lanzoni, B., Stoehr, F., Tormen, G., & Yoshida, N. 2004, *MNRAS*, 348, 333  
 D’Onghia, E., Besla, G., Cox, T. J., & Hernquist, L. 2009, *Nature*, 460, 605  
 Einasto, J., Saar, E., Kaasik, A., & Chernin, A. D. 1974, *Nature*, 252, 111  
 Faber, S. M. & Lin, D. N. C. 1983, *ApJ*, 266, L17  
 Geha, M., Blanton, M. R., Masjedi, M., & West, A. A. 2006, *ApJ*, 653, 240  
 Gottlöber, S., Hoffman, Y., & Yepes, G. 2010, in *Proceedings of "High Performance Computing in Science and Engineering, Garching/Munich 2009"*, Springer-Verlag (astro-ph/1005.2687)  
 Grcevich, J. & Putman, M. E. 2009, *ApJ*, 696, 385  
 Grebel, E. K. 2000, in *ESA Special Publication*, Vol. 445, *Star Formation from the Small to the Large Scale*, ed. F. Favata, A. Kaas, & A. Wilson, 87  
 Kaufmann, T., Wheeler, C., & Bullock, J. S. 2007, *MNRAS*, 382, 1187  
 Kazantzidis, S., Lokas, E. L., Callegari, S., Mayer, L., & Moustakas, L. A. 2011, *ApJ*, 726, 98  
 Kazantzidis, S. et al. 2005, *ApJ*, 623, L67  
 Klimentowski, J., Lokas, E. L., Kazantzidis, S., Mayer, L., & Mamon, G. A. 2009, *MNRAS*, 397, 2015  
 Klimentowski, J., Lokas, E. L., Knebe, A., Gottlöber, S., Martínez-Vaquero, L. A., Yepes, G., & Hoffman, Y. 2010, *MNRAS*, 402, 1899  
 Knebe, A., Power, C., Gill, S. P. D., & Gibson, B. K. 2006, *MNRAS*, 368, 741  
 Knollmann, S. R. & Knebe, A. 2009, *ApJS*, 182, 608  
 Kopylov, A. I., Tikhonov, N. A., Fabrika, S., Drozdovsky, I., & Valeev, A. F. 2008, *MNRAS*, 387, L45  
 Kravtsov, A. V., Gnedin, O. Y., & Klypin, A. A. 2004, *ApJ*, 609, 482  
 Lokas, E. L. 2009, *MNRAS*, 394, L102  
 Lokas, E. L., Kazantzidis, S., & Mayer, L. 2011, *ApJ* accepted (astro-ph/1103.4909)  
 Ludlow, A. D., Navarro, J. F., Springel, V., Jenkins, A., Frenk, C. S., & Helmi, A. 2009, *ApJ*, 692, 931  
 Mateo, M. L. 1998, *ARA&A*, 36, 435  
 Mayer, L. 2010, *Advances in Astronomy*, vol. 2010, Article ID 278434 (astro-ph/0909.4075), 1  
 Mayer, L., Governato, F., Colpi, M., Moore, B., Quinn, T., Wadsley, J., Stadel, J., & Lake, G. 2001, *ApJ*, 559, 754  
 Mayer, L., Kazantzidis, S., Mastropietro, C., & Wadsley, J. 2007, *Nature*, 445, 738  
 Mayer, L., Mastropietro, C., Wadsley, J., Stadel, J., & Moore, B. 2006, *MNRAS*, 369, 1021  
 McConnachie, A. W. & Irwin, M. J. 2006, *MNRAS*, 365, 1263  
 McConnachie, A. W., Irwin, M. J., Ferguson, A. M. N., Ibata, R. A., Lewis, G. F., & Tanvir, N. 2005, *MNRAS*, 356, 979  
 McGaugh, S. S. & Wolf, J. 2010, *ApJ*, 722, 248  
 Mo, H. J., Mao, S., & White, S. D. M. 1998, *MNRAS*, 295, 319  
 Monelli, M., Cassisi, S., Bernard, E. J., Hidalgo, S. L., Aparicio, A., Gallart, C., & Skillman, E. D. 2010a, *ApJ*, 718, 707  
 Monelli, M. et al. 2010b, *ApJ*, 720, 1225  
 Navarro, J. F., Frenk, C. S., & White, S. D. M. 1996, *ApJ*, 462, 563  
 Oh, S.-H. et al. 2011, *AJ*, 142, 24  
 Peebles, P. J. E. 1969, *ApJ*, 155, 393  
 Sales, L. V., Navarro, J. F., Abadi, M. G., & Steinmetz, M. 2007, *MNRAS*, 379, 1475  
 Saviane, I., Held, E. V., & Piotto, G. 1996, *A&A*, 315, 40  
 Stadel, J. G. 2001, Ph.D. Thesis, Univ. of Washington  
 Susa, H. & Umemura, M. 2004, *ApJ*, 610, L5  
 Tolstoy, E., Hill, V., & Tosi, M. 2009, *ARA&A*, 47, 371  
 Walker, M. G., Mateo, M., Olszewski, E. W., Peñarrubia, J., Evans, N. W., & Gilmore, G. 2009, *ApJ*, 704, 1274  
 Wechsler, R. H., Bullock, J. S., Primack, J. R., Kravtsov, A. V., & Dekel, A. 2002, *ApJ*, 568, 52

- White, S. D. M. & Rees, M. J. 1978, MNRAS, 183, 341  
Young, L. M. & Lo, K. Y. 1997, ApJ, 490, 710